COMPUTATION OF BROADBAND, HIGH-POWER ELECTROMAGNETIC PULSE GENERATION FROM AN AIR GAS AVALANCHE SWITCH*

D.J. Mayhall and J.H. Yee
Lawrence Livermore National Laboratory
University of California
P.O. Box 808, Mail Code L-156
Livermore, CA 94551

Abstract

A two-dimensional, electromagnetic, electron fluid computer code predicts picosecond-scale electromagnetic wave generation in a simple air avalanche switch. Similar pulses occur from kilovolts to megavolts for proper scaling of the pressure. At fixed voltage, the pulse width varies with pressure. At fixed pressure, the pulse width varies with voltage. The pulse width can be reduced to 1–2 ps by operation in the wave interference mode. In this mode, one air gap fires with a slight delay from the other air gap. This delay is some fraction of a picosecond.

Introduction

The gas avalanche switch, a high-voltage, high-pressure, picosecond-speed switch has recently been proposed [1]. The basic switch consists of a set of pulse-charged electrodes, immersed in a high-pressure (2–800 atm) gas. An avalanche discharge is initiated in the gas between the electrodes by ionization from a picosecond-scale laser pulse. The electrons rapidly avalanche toward the anode in the applied field. This avalanche, fueled by the immense number of electrons available in the gas, causes the applied voltage to collapse within picoseconds.

Several versions of the switch are possible. A parallel plate capacitor version consists of a gas confined between two flat parallel plates. Cylindrical coaxial versions are also possible. A simple pulse generator variant has a center electrode between two horizontal parallel plates. In this case, the center electrode is charged to a suitable, positive high voltage, and the gap between this electrode and one of the plates is rapidly illuminated with suitable laser light. If the ensuring voltage collapse is rapid enough, it generates predominantly TEM waves, which move outward from the center electrode. For investigation of the generation and propagation of these waves in gas avalanche switches, we have developed a two-dimensional, electromagnetic, electron fluid code, which includes avalanche ionization.

The Two-Dimensional, Electromagnetic, Electron Fluid Computer Code

The computer code simultaneously and self-consistently solves Maxwell's curl equations for transverse electromagnetic (TM) modes in a gas between perfectly conducting parallel plates. In addition, it solves electron fluid conversation equations for continuity, momentum, and energy. Rectilinear perfect conductors may be suspended between the plates.

For a free space dielectric, Maxwell's equations in MKS are

$$\frac{\partial \mathbf{E_x}}{\partial t} = \varepsilon_0^{-1}\left(\frac{\partial \mathbf{H_z}}{\partial y} - \mathbf{ne}\mathbf{v_x}\right) , \tag{1}$$

$$\frac{\partial \mathbf{E_y}}{\partial t} = -\varepsilon_0^{-1}\left(\frac{\partial \mathbf{H_z}}{\partial x} + \mathbf{ne}\mathbf{v_y}\right) , \tag{2}$$

$$\frac{\partial \mathbf{H_z}}{\partial t} = \mu_0^{-1}\left(\frac{\partial \mathbf{E_x}}{\partial y} - \frac{\partial \mathbf{E_y}}{\partial x}\right) , \tag{3}$$

where E_x and E_y are the electric field components in the x and y directions, ε_0 and μ_0 are the permittivity and permeability, H_z is the magnetic component in the z direction, n is the electron density, v_x and v_y are the velocity components in the x and y directions, and e is the electron charge, -1.6×10^{-19} C.

The electron fluid conservation equations are

$$\frac{\partial \mathbf{n}}{\partial t} = \mathbf{n}\nu_i , \tag{4}$$

$$\frac{\partial (\mathbf{n}\mathbf{v_x})}{\partial t} = \mathbf{n}\left(\mathbf{e}\mathbf{m}^{-1}\mathbf{E_x} - \nu_m \mathbf{v_x}\right) , \tag{5}$$

$$\frac{\partial (\mathbf{n}\mathbf{v_y})}{\partial t} = \mathbf{n}\left(\mathbf{e}\mathbf{m}^{-1}\mathbf{E_y} - \nu_m \mathbf{v_y}\right) , \tag{6}$$

$$\frac{\partial (\mathbf{nU})}{\partial t} = \mathbf{n}\left[\mathbf{e}\left(\mathbf{E_x}\mathbf{v_x} + \mathbf{E_y}\mathbf{v_y}\right) - \nu_u\left(\mathbf{U} - \mathbf{U_0}\right) - \nu_i \varepsilon_i\right] , \tag{7}$$

where ν_i is the ionization collision frequency, m is the electron mass, ν_m and ν_u are the electron-neutral molecule momentum and energy transfer collision frequencies, U is the electron energy, U_0 is the average neutral energy, and ε_i is the average neutral ionization potential. For air, we take $U_0 = 0.025$ eV and $\varepsilon_i = 14$ eV. Convection, magnetic forces, pressure gradients, and heat flows are neglected. Diffusive and all atomic and molecular electron number losses are also neglected. Electron generation from photoionization is ignored. The collision frequencies are those used previously in microwave air breakdown calculations [2,3]. The collision frequencies are assumed to scale directly with pressure. In addition, electrode pulse charging and laser-driven electron deposition are assumed to be instantaneous.

The space between the plates is partitioned with a regular rectangular computational mesh with spacings Δx and Δy in the x and y directions, respectively. These spacings may be unequal. Grid points for the seven solution variables are selected to obtain the type of staggered grid used in explicit, finite difference, electromagnetic scattering codes [4]. E_x is placed at even grid points on odd horizontal (xz) planes. The bottom of these is the top surface of the lower conducting plate. The uppermost is the bottom surface of the top plate. E_y is located at odd grid points on even horizontal plates. H_z is located at even points on the same planes. The four electron fluid variables reside at the H_z points. The spatial derivatives are approximated by central finite differences in the grid interior and one-sided differences on and near the boundaries. The left side time derivatives of fluid variable products in Eqs. (5)–(7) are expanded, and Eq. (4) is substituted. The resulting discretized global set of ordinary differential equations is solved by time integration with the block-iterative, optionally stiff, implicit, variable step solver GEARBI [5].

The Elementary Pulse Generator Switch

An elementary pulse generator switch can be created by placing a single properly shaped and dimensioned electrode between parallel plates. When this center electrode is charged to the correct positive high voltage, V_o, the lower gap is bridged with laser-generated electrons, and a suitable air pressure is specified, electromagnetic waves of picosecond rise times and durations occur. Figure 1 shows a computational model of this switch. The lower gap is uniformly filled with 1.7×10^{13} electrons to an

*Work performed under the auspices of the U.S. Department of Energy by Lawrence Livermore National Laboratory under Contract W-7405-Eng-48.

Report Documentation Page

Form Approved
OMB No. 0704-0188

1. REPORT DATE	2. REPORT TYPE	3. DATES COVERED
JUN 1991	**N/A**	**-**

4. TITLE AND SUBTITLE
Computation Of Broadband, High-Power Electromagnetic Pulse Generation From An Air Gas Avalanche Switch

5a. CONTRACT NUMBER
5b. GRANT NUMBER
5c. PROGRAM ELEMENT NUMBER

6. AUTHOR(S)

5d. PROJECT NUMBER
5e. TASK NUMBER
5f. WORK UNIT NUMBER

7. PERFORMING ORGANIZATION NAME(S) AND ADDRESS(ES)
Lawrence Livermore National Laboratory University of California P.O. Box 808, Mail Code L-156 Livermore, CA 94551.

8. PERFORMING ORGANIZATION REPORT NUMBER

9. SPONSORING/MONITORING AGENCY NAME(S) AND ADDRESS(ES)

10. SPONSOR/MONITOR'S ACRONYM(S)

11. SPONSOR/MONITOR'S REPORT NUMBER(S)

12. DISTRIBUTION/AVAILABILITY STATEMENT
Approved for public release, distribution unlimited

13. SUPPLEMENTARY NOTES
See also ADM002371. 2013 IEEE Pulsed Power Conference, Digest of Technical Papers 1976-2013, and Abstracts of the 2013 IEEE International Conference on Plasma Science. Held in San Francisco, CA on 16-21 June 2013. U.S. Government or Federal Purpose Rights License

14. ABSTRACT
A two-dimensional, electromagnetic, electron fluid computer code predicts picosecond-scale electromagnetic wave generation in a simple air avalanche switch. Similar pulses occur from kilovolts to IT\egavolts for proper scaling of the pressure. At fixed voltage, the pulse width varies with pressure. At fixed pressure, the pulse width varies with voltage. The pulse width can be reduced to 1-2 ps by operation in the wave interference mode. In this mode, one air gap fires with a slight delay from the other air gap. This delay is some fraction of a picosecond.

15. SUBJECT TERMS

16. SECURITY CLASSIFICATION OF:			17. LIMITATION OF ABSTRACT	18. NUMBER OF PAGES	19a. NAME OF RESPONSIBLE PERSON
a. REPORT	b. ABSTRACT	c. THIS PAGE			
unclassified	**unclassified**	**unclassified**	**SAR**	**4**	

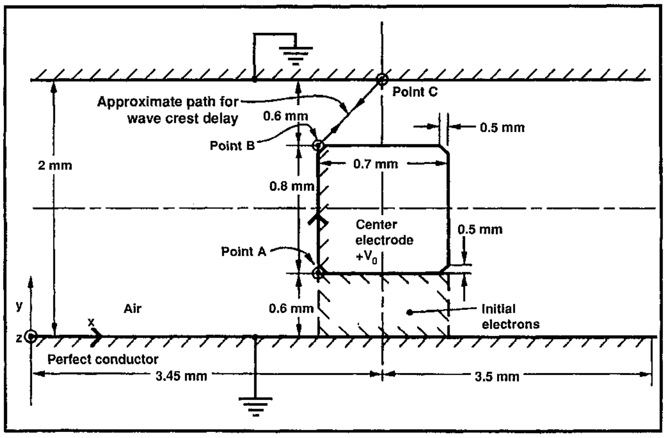

Figure 1. The pulse generator switch model.

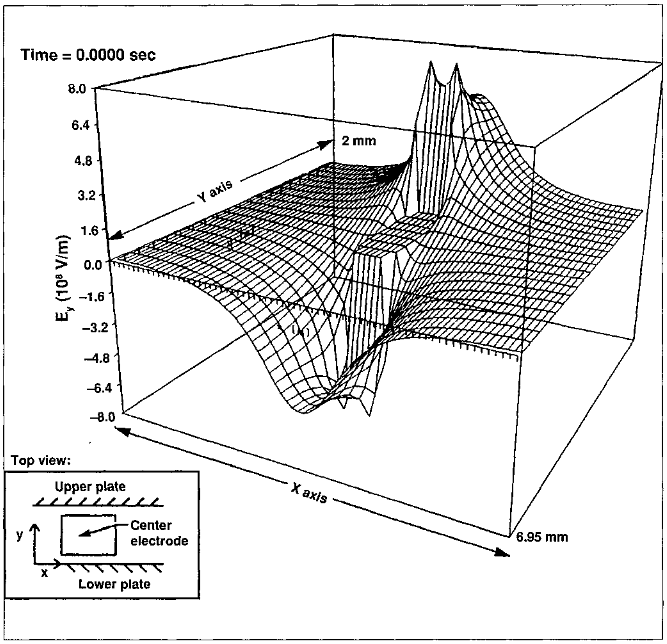

Figure 2. Initial distribution of E_y.

assumed depth of 1 m into the figure.

The initial electric components are obtained from the finite element, electrostatic code STAT2D and used as initial conditions for the electron fluid code. Figure 2 shows the initial distribution of E_y. After the simulation starts, the voltage across the lower gap collapses rapidly. Figure 3 displays this collapse near the vertical center line for 292 kV on the center electrode and 27.2 atm of pressure. The voltage falls to ~20% of its initial absolute value in about 3 ps. It then trails off more slowly to zero over about 25 ps. Avalanche-generated E_y waves move out from the left and right ends of the center electrode and exit the computational space at the two vertical boundaries. These waves induce dynamic voltages between the plates. Figure 4a shows the voltage waveform at the right boundary, calculated from the line integral of E_y. The delay to the pulse rise is 10.5 ps, the peak voltage is 300 kV, the 10–90% rise time to that peak is 2.41 ps, the FWHM is 9.11 ps, and the pulse duration exceeds 20 ps. The initial electrostatic energy is 3.34 J/m. By 36.5 ps, 55.4% of the initial energy has crossed the free space boundaries. The peak pulse voltage represents a 2.67% enhancement of the initial applied voltage. The tail of the voltage pulse appears to be due to a slow decay of a residual electric field in the upper gap. This decay could most likely be greatly accelerated with a delayed illumination of that gap. The first peak of the waveform is from the crest of the wave along the bottom plate; the second peak is from lagging wave crests in the interior space and along the top plate.

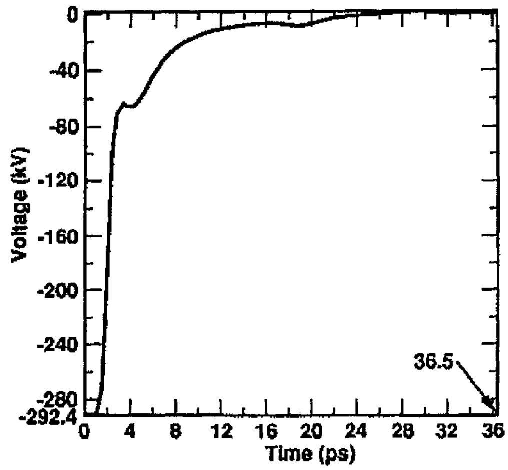

Figure 3. Waveform of the voltage between the center electrode and the bottom plate near the vertical center line.

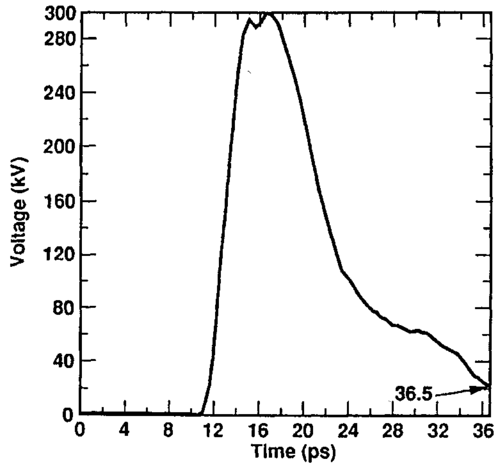

Figure 4a. Voltage waveform at right boundary at 292.4 kV and 27.2 atm.

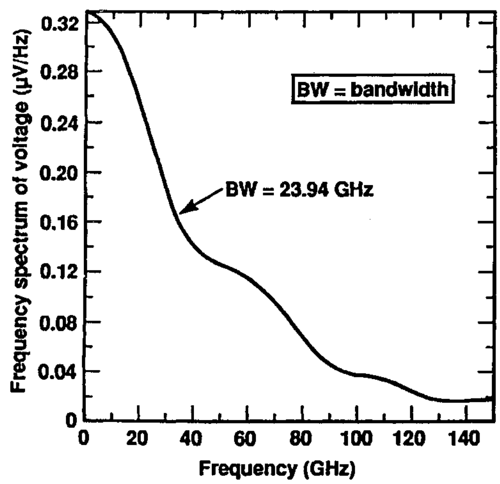

Figure 4b. Frequency spectrum of the voltage at 292.4 kV and 27.2 atm.

Figure 4b shows the spectrum of the voltage pulse. The spectral peak is at dc, and the 3 dB bandwidth is 23.9 GHz. This result assumes that the induced voltage drops abruptly to zero at 36.5 ps. Figure 5a shows the waveform of the outwardly directed instantaneous electromagnetic power at the right boundary. The rise time is 2.79 ps, the FWHM is 6.49 ps, and the duration is ~25.5 ps. The peak power is 0.128 TW per meter depth of the center electrode. The frequency spectrum of this

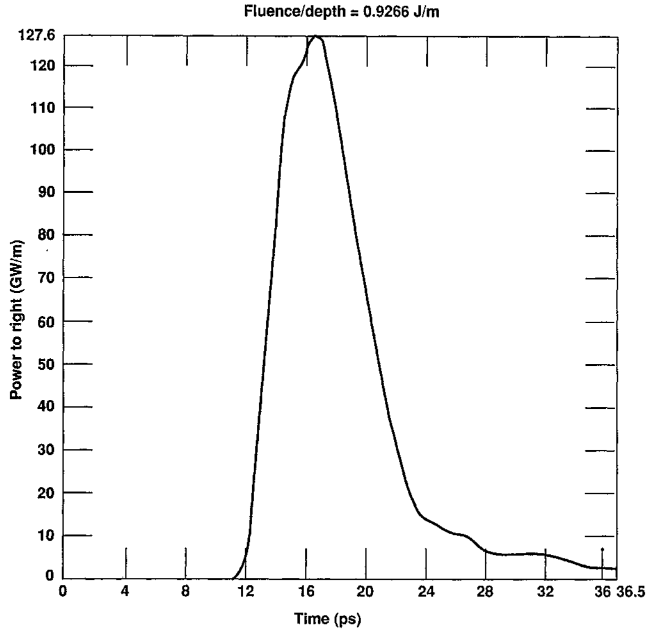

Figure 5a. Instantaneous power across right boundary.

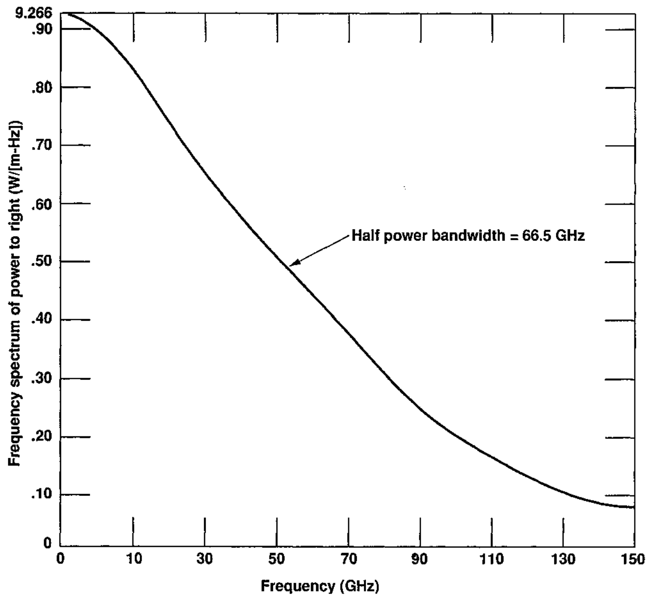

Figure 5b. Frequency spectrum of the instantaneous power across right boundary.

instantaneous power waveform is shown in Fig. 5b. The 3 dB bandwidth, that is, the spectral width at the half power points, is 66.5 GHz. The bandwidth of the electromagnetic power transmitted to the right is 2.51 times the bandwidth of the induced voltage pulse.

Very similar pulses occur at 3.89 MV and 750 atm [6] and at 227 kV and 15.2 atm. At the latter voltage and pressure, induced voltage pulses occur with peaks of 241 kV, rise times of 2.28 ps, FWHMs of 8.38 ps, durations of about 30 ps, and 3 dB bandwidths of 24 GHz.

At fixed voltage, shorter pulse widths can be obtained by decreasing the pressure. This increases the initial E_y at the center electrode and speeds up the avalanche and the ensuring voltage collapse. Table 1 shows the variation of several characteristics of the right side voltage pulse at 227 kV as the pressure varies from 17–1 atm. The rise time drops by 41% and the FWHM drops by 21%.

Table 1. Variation of right side voltage pulse characteristics with air pressure at 227 kV center electrode voltage

Air pressure (atm)	Rise time (ps)	FWHM (ps)	Peak voltage (kV)	3 db bandwidth (GHz)
17	2.56	8.98	236.6	26.9
15	2.28	8.38	240.5	23.9
7	1.87	7.57	264.2	39.6
1	1.51	7.12	277.7	42.5

At fixed voltage, longer pulse widths can be obtained by increasing the pressure. At fixed pressure, longer pulse widths can be generated by decreasing the applied voltage. Table 2 shows several right side induced voltage pulse characteristics for reduction of the center electrode voltage. The pressure is roughly constant at 8 atm. The pulse FWHM increases from 7.57–167 ps, and the 3 dB bandwidth decreases from 39.6–1.71 GHz.

Table 2. Variation of right side voltage pulse characteristics with voltage at roughly 8 atm air pressure

Air pressure (atm)	Applied voltage (kV)	Rise time (ps)	FWHM (ps)	Duration (ps)	Peak voltage (kV)	Bandwidth (GHz)
17	227	1.87	7.57	>15.5	264.2	39.6
15	48.8	14.7	28.9	>109	18.5	9.28
7	24.4	20.1	167	>385	1.71	1.71

Operation in the Wave Interference Mode

At fixed voltage, a modest reduction in pulse width occurs from reduction of the air pressure. For given physical dimensions, the minimal pulse width must be limited by some critical dimensions. The delay in the arrival of the wave crests along the lower and upper parallel plates partially determines the induced voltage pulse width. This delay probably depends on a path difference like that from point A in Fig. 1 to point B to point C and back to point B. This trajectory is defined in Fig. 1 by the arrowheads. Use of this path difference and the speed of light in vacuum gives a delay of 7.3 ps. This is close to the pulse FWHM of 7.12 ps given in Table 1. The sizes of the center electrode and the air gap limit the minimum obtainable pulse width. Reduction of these critical dimensions should reduce the pulse width.

There is another way to reduce the width of the induced voltage pulse without reducing the pressure or the critical device dimensions. This is to fire the upper air gap slightly after the lower gap. If the avalanches in the two gaps are roughly similar, two roughly equal, but oppositely polarized rightwardly traveling waves arise at the gaps. For the positively charged center electrode, the wave from the lower gap is positive, and that from the upper gap is negative. With no firing delay the two electromagnetic waves should interfere destructively at the right boundary to cancel almost completely. This cancellation should result in virtually no induced voltage at the boundary. With the firing of the upper gap delayed slightly from the firing of the lower gap, the negative wave from the upper gap should cancel only the tail of the wave from the lower gap. Electromagnetic wave interference thus will reduce the width of the voltage pulse.

Figure 6 shows two right side voltage pulses generated by wave interference. An electron number of 1.7×10^{13} electrons/m depth uniformly fills each gap. The center electrode voltage is 227 kV. The pressure is 15 atm. The delay is 0.5 ps for the left waveform, which has an amplitude of 51.1 kV and a FWHM of 1.79 ps. This pulse has a very slight negative precursor and an irregular trailing tail of about 7 kV amplitude. The price for a shorter main pulse is a dramatic amplitude reduction. Figure 7a shows the frequency spectrum of this pulse. The bandwidth is 113 GHz. This large value occurs because the 0.707 upper spectral cut off value falls just below the spectral dips at about 60 and

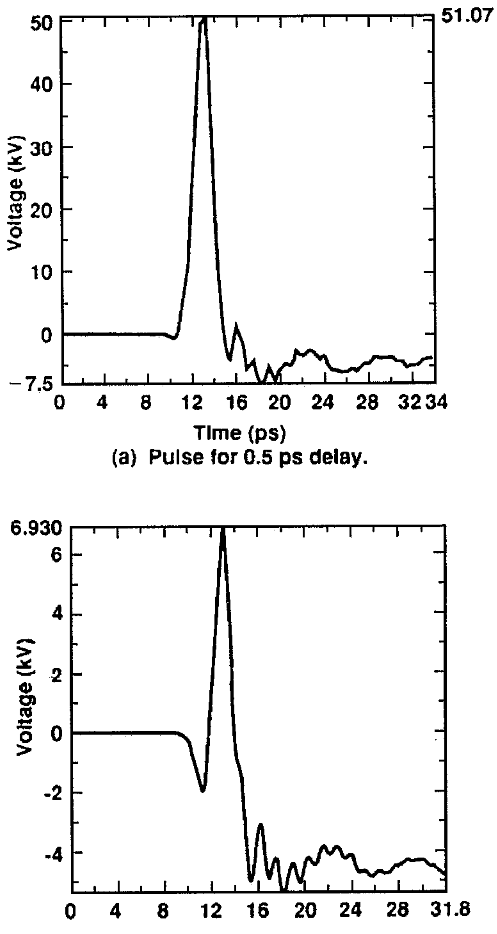

(a) Pulse for 0.5 ps delay.

(b) Pulse for 0.1 ps delay.

Figure 6. Voltage waveforms generated by wave interference.

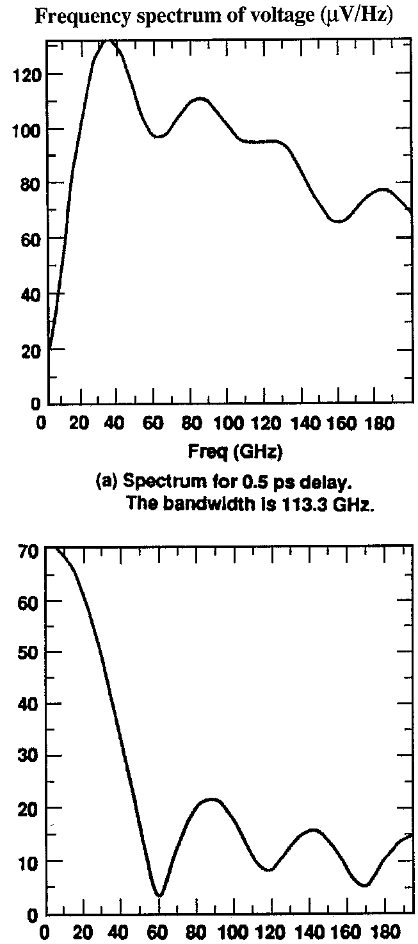

(a) Spectrum for 0.5 ps delay.
The bandwidth is 113.3 GHz.

(b) Spectrum for 0.1 ps delay.
The bandwidth is 28.09 GHz.

Figure 7. Voltage spectra generated by wave interference.

100 GHz. A shorter delay of 0.1 ps produces the voltage waveform in Fig. 6b. Because of the stronger interference, this pulse has a lower peak of 6.93 kV and a shorter FWHM of 1.14 ps. Unfortunately, this pulse also has a negative precursor of about −2 kV and a prominent negative trailing signal with an amplitude of about 5.3 kV. The peak value of the main pulse is only 3.05% of the applied voltage. The spectrum of this waveform is shown in Fig. 7b. The bandwidth is 28.1 GHz. This bandwidth is less than that of 0.5 ps delay because of the strong trailing signal. Strong attenuation of this signal should greatly increase the bandwidth.

Conclusions

A two-dimensional, electromagnetic, electron fluid computer code investigation of a simple pulse generator air avalanche switch predicts high-voltage (227 kV–4 MV), wideband (20 GHz) electromagnetic pulses with picosecond rise times and durations. At fixed center electrode voltage, the pulse width may be modestly reduced by pressure reduction. At fixed pressure, the pulse width may be increased by voltage reduction. The pulse characteristics are thus easily tunable with the physical dimensions fixed. Similar pulses can be produced over a wide range of voltage as long as the initial voltage to pressure ratio is roughly constant. The pulse width can be dramatically reduced in the wave interference mode of operation. The laser-activated, air avalanche switch computationally shows great promise for the generation of high-voltage, wideband electromagnetic pulses.

References

[1] R.E. Cassell and F. Villa, "High Speed Switching In Gases," SLAC-PUB-4858, February 1989.

[2] J.H. Yee, R.A. Alvarez, D.J. Mayhall, D.P. Byrne, and J. DeGroot, "Theory of Short, Intense Electromagnetic Pulse Propagation Through the Atmosphere," Phys. Fluids, vol. 29, pp. 1238–1244, April 1986.

[3] G.E. Sieger, J.H. Yee, and D.J. Mayhall, "Computer Simulation of Nonlinear Coupling of High-Power Microwaves with Slots," IEEE Trans. Plasma Science, vol. 17, pp. 616–621, August 1989.

[4] K.S. Yee, "Numerical Simulation of Initial Boundary Value Problems Involving Maxwell's Equations in Isotropic Media," IEEE Trans. Ant. and Propagat., vol. AP-14, pp. 302–307, 1966.

[5] A.C. Hindmarsh, "Preliminary Documentation of GEARBI: Solution of ODE Systems with Block-Iterative Treatment of the Jacobian," UCID-30149, Lawrence Livermore National Laboratory, Livermore, CA , 1976.

[6] D.J. Mayhall, J.H. Yee, and F. Villa, "Computer Code Prediction of Picosecond Voltage Switching and TEM Wave Generation in Air Gas Avalanche Switches," in Proc. of IEEE 7th Pulsed Power Conference, Monterey, CA, June 11–14, 1989, pp. 514–517.